

Environmental Science Processes & Impacts

Accepted Manuscript



This is an *Accepted Manuscript*, which has been through the Royal Society of Chemistry peer review process and has been accepted for publication.

Accepted Manuscripts are published online shortly after acceptance, before technical editing, formatting and proof reading. Using this free service, authors can make their results available to the community, in citable form, before we publish the edited article. We will replace this *Accepted Manuscript* with the edited and formatted *Advance Article* as soon as it is available.

You can find more information about *Accepted Manuscripts* in the [Information for Authors](#).

Please note that technical editing may introduce minor changes to the text and/or graphics, which may alter content. The journal's standard [Terms & Conditions](#) and the [Ethical guidelines](#) still apply. In no event shall the Royal Society of Chemistry be held responsible for any errors or omissions in this *Accepted Manuscript* or any consequences arising from the use of any information it contains.

Environmental impact

The use of biofuels has the potential to decrease greenhouse gas emissions. The potential for environmental risk should be accounted for. A laboratory study was undertaken for predicting the fate and transport of hydrophobic organic compounds in the subsurface in the event of a biofuel spill. The spill scenarios generated can assist in the assessment of biofuel-contaminated sites.

Assessing Soil and Groundwater Contamination from Biofuel Spills

Colin S. Chen^a, Youn-Yuen Shu^b, Suh-Huey Wu^c, Chien-Jung Tien^{a*}

^a Department of Biotechnology, National Kaohsiung Normal University, Kaohsiung 824, Taiwan.

^b Department of Chemistry, National Kaohsiung Normal University, Kaohsiung 824, Taiwan.

^c Department of Safety, Health and Environmental Engineering, National United University, Miaoli 350, Taiwan.

Corresponding author.
Chien-Jung Tien, Ph.D.
Professor
Department of Biotechnology
National Kaohsiung Normal University
62, Shen-Chung Rd., Yanchao
Kaohsiung 824, Taiwan
Phone: 886-77172930 ext. 7318
Fax: 886-7605-1353
E-mail: cjtien@nkn.edu.tw

Revision prepared for submission to:

Environmental Science: Processes & Impacts

December 20, 2014

1 Abstract

2 Future modifications of fuels should include evaluations of the proposed constituents for
3 their potential to damage environmental resources such as the subsurface environment.

4 Batch and column experiments were designed to simulate biofuel spills in the subsurface
5 environment and to evaluate the sorption and desorption behavior of target fuel constituents
6 (i.e., monoaromatic and polyaromatic hydrocarbons) in soil. The extent and reversibility of
7 the sorption of aromatic biofuel constituents onto soil were determined. When the ethanol
8 content in ethanol-blended gasoline exceeded 25%, enhanced desorption of the aromatic
9 constituents to water was observed. However, when biodiesel was added to diesel fuel, the
10 sorption of target compounds was not affected. In addition, when the organic carbon
11 content of the soil was higher, the desorption of target compounds into water was lower.

12 The empirical relationships between the organic-carbon normalized sorption coefficient (K_{oc})
13 and water solubility and between K_{oc} and the octanol-water partition coefficient (K_{ow}) were
14 established. Column experiments were carried out for the comparison of column effluent
15 concentration/mass from biofuel-contaminated soil. The dissolution of target components
16 depended on chemical properties such as hydrophobicity and total mass of biofuel. This study
17 provides a basis for predicting the fate and transport of hydrophobic organic compounds in
18 the event of a biofuel spill. The spill scenarios generated can assist in the assessment of
19 biofuel-contaminated sites.

20

21 Keywords: sorption, cosolvent effect, ethanol-blended gasoline, biodiesel

22

23

24 1. Introduction

25 In the present energetic context, diversifying fuel sources has become essential for
26 meeting the growing world energy demand in a sustainable way. Biofuels derived from
27 renewable resources represent an attractive source of energy because they generate a smaller
28 greenhouse effect than fossil fuels. Such an objective implies the conversion of biomass
29 into biofuels. The biofuels that are currently available are ethanol and ethyl tert-butyl ether
30 (ETBE) for gasoline engines and biodiesel for diesel applications, which is produced from the
31 trans-esterification of vegetable oils. Ethanol can be mixed with conventional gasoline and
32 biodiesel with fossil diesel to different concentrations.

33 As biofuels are becoming widely used, their fate in the subsurface environment is an
34 area of concern. For instance, ethanol is blended into gasoline to add octane and oxygen,
35 and it may help reduce certain types of emissions. However, ethanol is water miscible; once
36 ethanol-blended gasoline spills occur, ethanol will be at the front of the contaminant plume.¹⁻⁴
37 Therefore, ethanol tends to be attenuated in the unsaturated zone and in groundwater.^{2,3}
38 Previous batch equilibrium experiments have indicated that the concentrations of benzene,
39 toluene, xylene and other hydrocarbons can be significantly enhanced when the ethanol
40 concentration in the aqueous phase is greater than 10% (v/v).⁵⁻⁸ Benzene was enhanced by a
41 factor of 1.2 at 10 vol% ethanol.⁵ Enhancements increased in proportion to the ethanol
42 concentration, and enhancements were much greater for lower solubility compounds (e.g.,
43 enhancement for 1,2,4-trimethylbenzene >> benzene).⁵⁻⁸ Additionally, ethanol may reduce
44 the biodegradation rates of aromatic fuel components in the subsurface in both transient and
45 near steady-state conditions.⁹⁻¹²

46 Variability in the biofuel-water partitioning of major aromatic constituents (i.e.,
47 benzene, toluene, ethylbenzene, and xylene (BTEX)) and methyl tert-butyl ether (MTBE)
48 have been examined for ethanol-blended gasoline.⁸ Ethanol at low percentages (below 5%),

49 was shown to have minimal or negligible cosolvent effects on hydrocarbon partitioning.⁶ In
50 the case of high fuel-to-water ratios (e.g., 1:1) or near the contaminant source zone, the
51 cosolvent effect of gasoline with high ethanol content (e.g., 85%) is environmentally
52 significant.^{5,7,8}

53 Biodiesel is used to formulate a range of mixtures from 1% biodiesel blended with 99%
54 fossil diesel to pure FAME (100% biodiesel), and is known by the percentage of biodiesel
55 with a B-prefix. Since current blends typically range from 1% (B1) to 20% (B20) biodiesel,
56 the partition coefficients of polynuclear aromatic hydrocarbons (PAHs) between biodiesel
57 fuel mixtures (i.e., B1, B5, and B20) and water were determined.¹³ Models were derived
58 using the Raoult's law convention for the activity coefficients and the liquid solubility. The
59 observed inverse, log-log linear dependence of the biodiesel-water partition coefficients of
60 target compounds on the aqueous solubility were well predicted by assuming biodiesel to be
61 an ideal solvent mixture.¹³ The experimental partition coefficients were compared with
62 calculations by polyparameter linear free energy relationship (PP-LFER) approaches. The
63 experimental partition coefficients were generally well reproduced by PP-LFER.¹³

64 The chemical composition of biofuel products is complex and may change over time
65 following release into the environment. Biofuel components might contaminate drinking
66 water resources as a result of transfer from released constituents to groundwater followed by
67 advective transport to a public or private well. However, most biofuel constituents are only
68 weakly soluble in water and highly sorptive to aquifer solids. Therefore they are retarded
69 with respect to groundwater flow or substantially biodegraded in the subsurface before
70 migration to drinking water wells.

71 Risk-based analyses of biofuel-contaminated sites is hampered by a lack of readily
72 available knowledge describing the fate and transport of biofuel products in the subsurface
73 environment. This problem is magnified by biofuel additives. A thorough understanding

74 of the environmental behavior of biofuels and the influence that biofuel additives may have
75 on the fate of other fuel constituents is needed. Thus, the objectives of this study were to (1)
76 investigate the desorption of aromatic constituents from biofuel-contaminated soils, (2) assess
77 any cosolvent effects of ethanol on the sorption of major components when a biofuel spill
78 occurs, and (3) evaluate the leaching pattern of contaminants from biofuel-contaminated soil
79 in the subsurface environment.

80

81 **Materials and Methods**

82 *Biofuel products*

83 The biofuels investigated in this study were ethanol-blended gasoline and biodiesel fuel.
84 The E3 (gasoline with 3% ethanol), regular gasoline (research octane number 95), and B1
85 (1% biodiesel blended with 99% fossil diesel) were obtained from a major supplier (i.e.,
86 Chinese Petroleum Corporation (CPC)) in Kaohsiung, Taiwan. Ethanol-blended gasoline
87 containing 10, 25, and 85% ethanol, respectively, was prepared by mixing regular gasoline
88 (research octane number 95, CPC 95) and ethanol in the laboratory. B100 biodiesel was
89 obtained from a production plant in southern Taiwan. B5 and B20 biodiesel were prepared
90 by mixing the proper volumes of diesel and biodiesel fuels in the laboratory. The fuel
91 products were transferred to different glass containers with Teflon-lined caps and stored in
92 the dark at 4°C.

93

94 *Biofuel-contaminated soils*

95 The soil samples used in this study were collected in Kaohsiung, Taiwan. Upon receipt,
96 the samples were wet-sieved through a 2 mm sieve, homogenized, and stored at 4°C in glass
97 bottles with Teflon[®] lined caps. The samples were labeled S-1, S-2, and S-3. The physical
98 and chemical properties of the soil samples were determined prior to initiation of the

99 experiments. The moisture content of the soil samples was determined by weighing
100 approximately 10 g of soil before and after oven drying at 105°C for 24 hours. For the soils
101 used, the moisture contents were 1, 3, and 12%, respectively (dry weight basis). Soil
102 particle size distribution was determined using the hydrometer method.¹⁴ Soil S1 contained
103 77% sand, 16% silt, and 7% clay. Soil S2 consisted of 70% sand, 21% silt, and 9% clay.
104 Soil S3 was composed of 66% sand, 22% silt, and 12% clay. All the soil texture fell into
105 sandy loam. Organic carbon was determined by the Walkley-Black procedure with manual
106 titrimetric quantitation. The three soil samples (S-1, S-2, and S-3) with organic carbon
107 contents of 2.6, 4.5, and 10% were prepared for sorption studies.

108 To ensure that sorption reached equilibrium in a reasonable time, a preliminary study
109 was conducted to determine the proper equilibration time when biofuels contact soil. It was
110 found that 24 hours was suitable for the constituents of ethanol-blended gasoline and
111 biodiesel to reach equilibrium with soil. Ethanol-blended gasoline-contaminated soil was
112 prepared by mixing 0.1, 0.5, or 1 mL of ethanol-blended gasoline with 10 g of soil and
113 shaking for 24 hours in the dark at a constant temperature (20°C) to represent different
114 contamination levels. Headspace in the vials was kept to a minimum.
115 Biodiesel-contaminated soil was prepared by mixing 2, 4, or 6 mL of biodiesel with
116 approximately 10 g of soil and shaking for 24 hours in the dark at constant temperature
117 (20°C).

118

119 *Batch sorption experiments*

120 The equilibrium concentrations of aromatics in soil/water systems were determined by
121 batch sorption experiments. The target aromatic compounds were BTEX and PAHs. The
122 experimental setup was run in six replicates. Approximately ten grams of
123 biofuel-contaminated soil was placed in a reaction vial containing 10 mL of deionized (D.I.)

124 water with 0.01 N calcium chloride to equilibrate for 24 hours on a shaker at room
125 temperature ($22\pm 2^\circ\text{C}$). The calcium chloride was used to improve soil particle coagulation
126 and settling after attaining equilibrium. After shaking, the aqueous and soil phases were
127 separated by centrifugation. Prior to analysis, the aqueous samples in ethanol-blended
128 gasoline/soil experiment were filtered with a $0.45\ \mu\text{m}$ PTFE filter, and 2 gram of soil sample
129 was extracted by adding 10 mL of methanol.

130 Soils from the biodiesel/soil experiment were extracted in triplicate using a batch
131 extraction method developed in earlier study.¹⁵ Approximately 5 g of soil was placed in a
132 35-mL Kimax tube and sequentially extracted with 1:1 v/v methanol-methylene chloride in the
133 biodiesel/soil experiment. The aqueous sample in the biodiesel/soil experiment was
134 extracted three times with 10 mL of methylene chloride. A sorption coefficient (K_p) that
135 expresses the relationship between a component's concentration in soil (C_s) and the aqueous
136 phase (C_w) was calculated for the target compounds:

$$137 \quad K_p = C_s/C_w \quad (1)$$

138

139 *Column experiments*

140 Spills of biofuel in the contaminated subsurface environment were simulated by column
141 experiments. The miscible displacement technique was adopted for all experiments.^{16,17}
142 This technique involves the displacement of a solution through a column packed with a
143 material of interest.¹⁷ In the spill experiments with ethanol-blended gasoline, stainless
144 columns (1.5 cm i.d., 6 cm in length) packed with soil were employed to simulate spills of
145 ethanol-blended gasoline in the subsurface environment. Each column was used for only one
146 spill experiment. The column was saturated by flushing with an aqueous 0.01 N CaCl_2
147 solution for three hours (approximately 20 to 25 pore volumes) under continuous flow
148 conditions with a flow rate of $0.576\ \text{mL}/\text{min}$. Once the soil was saturated, the column was

149 placed in a horizontal position to minimize density-driven flow patterns. An injection of 1
150 mL of ethanol-blended gasoline was applied to represent an ethanol-blended gasoline leak to the
151 subsurface environment. After stopping the injection of ethanol-blended gasoline, the column
152 was allowed to saturate for 48 hours. Water (containing 0.01 N CaCl₂) was pumped through
153 the column at a flow rate of 0.96 mL/min for three hours (approximately 43 to 45 pore volumes).
154 The effluent from the soil columns was collected continuously. The effluents were stored in 5
155 mL glass vials with Teflon[®] lined septa at 4°C before headspace GC/FID analysis.

156 Glass columns (4.8 cm i.d., 15 cm in length) (Kontes Scientific Glassware, New Jersey)
157 packed with soil were employed to simulate spills of biodiesel in the subsurface environment.
158 The columns had Teflon[®] endplate fittings that were held in place by screw caps. The
159 column was saturated by flushing with an aqueous 0.01 N CaCl₂ solution for four hours under
160 continuous flow conditions with a flow rate of 0.576 mL/min. A continuous injection of
161 biodiesel was applied to represent a biodiesel spill in the subsurface environment. Biodiesel
162 was injected into the column at a flow rate of 0.576 mL/min for seventy minutes (approximately
163 40 mL of biodiesel). After stopping the injection of biodiesel, the column was allowed to
164 saturate for 48 hours. Then, water (containing 0.01 N CaCl₂) was pumped through the column
165 at a flow rate of 0.96 mL/min for three hours. This represents groundwater flow past the
166 biodiesel spill site after biofuel leakage/spillage had stopped. The effluent from the soil
167 columns was collected continuously every 30 mL. The effluents were stored in 40 mL glass
168 vials with Teflon[®] lined septa at 4°C before PAH analysis. To assess the elution profile, zero
169 moment analysis was conducted to calculate the mass of hydrophobic organic compounds
170 (HOCs) mobilized by groundwater.

171

172 *Analysis of target compounds*

173 The aqueous and soil samples from the sorption and column studies of ethanol-blended

174 gasoline were analyzed by an Agilent 6850 gas chromatograph/flame ionization detector
175 (GC/FID) equipped with a Teledyne Tekmar HT3 static/dynamic headspace system
176 (Teledyne Tekmar, USA). The individual vials were heated to 85°C and allowed to
177 equilibrate for 50 min. Each sample was mixed by mechanical vibration for 5 min during
178 this equilibration period. Each vial was pressurized with helium carrier gas to a pressure of
179 10 psi. The transfer line temperature was 150°C. The total run time including pressurized
180 equilibration time, loop fill pressurization, and stabilization time was 55.2 min.

181 The aqueous samples from the sorption and column experiments with biodiesel were
182 filtered with a 0.45 µm PTFE filter and extracted three times with 10 mL of methylene
183 chloride. The extract was dried by passing it through a sodium sulfate column to remove
184 residual water, and the extract volume was concentrated to 3-5 mL using a rotary evaporator.
185 The extract volume was further reduced under a gentle stream of nitrogen to 1 mL. The
186 extracts were transferred to 1 mL crimp-seal vials and refrigerated (4°C) until analysis.

187 Biodiesel-contaminated soil samples from both experimental settings were extracted in
188 triplicate using a batch extraction method as described in the batch sorption experiment section.
189 A portion of each contaminated soil sample was spiked with a 0.5 mL solution of surrogate
190 compounds two hours prior to extraction as a quality control. The surrogate spiking
191 solution contained naphthalene-d₈, anthracene-d₁₀, perylene-d₁₂, 2-fluorobiphenyl, and
192 p-terphenyl-d₁₄. Each chemical was spiked into the soil at a level of 20 mg/kg. The subset
193 of soil samples spiked included one for each biodiesel sorption experiment.

194 The extracts were analyzed for PAHs by an Agilent 6890/5973 GC/MS. Analytical
195 separation was achieved with a 0.32 mm i.d., 30 meter, fused silica HP-5MS (5%
196 phenyl-95% di-methylpoly siloxane) column with a 0.25 µm film thickness (Agilent J & W,
197 USA). The temperature program included a 2 min hold time at 50°C, temperature ramping
198 at 20°C/min to 130°C followed by 3 min hold time, then temperature ramping at 12°C/min to

199 180°C, ramping at 7°C/min to 275°C, with a final ramp at 5°C to 300°C with 4 min hold time.
200 Helium was the carrier gas at a flow rate of approximately 1.0 mL/min. Both injector and
201 detector temperatures were maintained at 250°C. The acquisition parameters for the MSD
202 were as follows: mass range 50-400 amu, scan rate 5.46 s, acquisition time 35.74 min,
203 filament delay 180 sec, mass defect 100 amu/100 amu, background mass 45 amu, electron
204 energy 70 eV, electron multiplier voltage 1694 eV, and transfer line temperature 250°C.
205 Internal standard calibration was performed during GC/MS analyses. The internal standards
206 included naphthalene-d₈, acenaphthalene-d₁₀, phenanthrene-d₁₀, chrysene-d₁₂, and
207 perylene-d₁₂.

208

209 **Results and Discussion**

210 *Batch sorption experiments*

211 The results in Table 1 indicate that the BTEX and MTBE in ethanol-blended gasoline
212 were not sorbed to the soil matrix as strongly as the aliphatic components, and they were
213 more likely to contaminate larger water volumes. The sorption of HOCs is controlled by
214 contaminant characteristics such as solubility, polarity and the octanol-water partition
215 coefficient (K_{ow}).^{18,19} In addition, sorption is influenced by the characteristics of the fluid
216 medium and the organic matter content of the soil.¹⁹ Overall, the sorption coefficients of the
217 HOCs paralleled their hydrophobicity. The sorption coefficient of MTBE was the lowest
218 among the compounds investigated as anticipated. However, it should be noted that MTBE
219 is typically absent in ethanol-enriched fuels (i.e., E25 or E85). In most cases, the sorption
220 coefficients of the target compounds in regular gasoline onto soil were the highest in the
221 near-source zone (i.e., biofuel/soil/water ratio=1:1:1) due to its maximal content of target
222 compounds.

223 Previous studies indicated that ethanol-enriched gasoline has a greater impact on soil

224 and groundwater than regular gasoline due to a variety of effects.^{1,8,20} Ethanol-blended
225 gasoline also undergoes a phase separation on contact with water, with ethanol reverting to
226 the aqueous phase, increasing its volume. The effect of ethanol on sorption was more
227 observable at the higher fuel/soil/water ratios in this study. The K_p values decreased with
228 increasing levels of ethanol in the ethanol-blended gasoline. However, at the low
229 biofuel/soil/water ratio (1:10:10) representing residual ethanol-blended gasoline
230 contamination, the K_p values displayed greater variation than under near-source
231 contamination. The non-parametric Mann-Whitney U test (Wilcoxon Rank Sum W test) and
232 Kruskal-Wallis one-way ANOVA were generally used to compare outcomes between two and
233 more than two independent groups, respectively. Thus, these two tests were used to analyze
234 the difference in the sorption coefficients of the target compounds in the various gasoline
235 products ($p < 0.05$ as a significance level). A significant difference was found between
236 ethanol content and the sorption coefficients of target compounds ($p < 0.05$). Overall it was
237 observed that the addition of ethanol led to reduced sorption of target compounds by soil, and
238 therefore it may increase the spreading groundwater contamination.

239 The addition of cosolvents has been shown to increase the mass transfer rate in
240 sorption.²¹⁻²⁴ It is anticipated that ethanol will decrease the retardation and sorption
241 coefficients of target compounds in biofuels. For the sorption of HOCs from
242 aqueous-organic binary solvent mixtures, the sorption coefficient is predicted to decrease
243 exponentially as the fraction of organic solvent increases. A log-linear cosolvency model
244 has been established to relate the equilibrium sorption coefficient (K_p) to the volume fraction
245 of cosolvent in a binary mixed solvent.^{25,26} The equation is expressed as:

$$246 \quad \log K_{p,b} = \log K_{p,w} - \alpha\beta\sigma f_c \quad (2)$$

247 where $K_{p,b}$ and $K_{p,w}$ are the equilibrium sorption constants for binary solvent and aqueous
248 systems, respectively, α is a nonideality coefficient that accounts for cosolvent-sorbent

249 interactions, β accounts for water-cosolvent interaction, and σ is the cosolvency power of the
250 cosolvent.

251 The cosolvent effect of ethanol was evaluated by calculating cosolvency powers for
252 three soils. The cosolvent effect of ethanol on the sorption of MTBE was the smallest
253 ($\alpha\beta\sigma=0.92, 1.03, \text{ and } 2.51$, respectively, in the three soil samples) for the sorption of
254 ethanol-blended gasoline onto soil. The reduction in the $K_{p,b}$ of benzene under the influence
255 of ethanol was the highest ($\alpha\beta\sigma=2.82, 3.13, \text{ and } 4.22$, respectively, in the three soil samples).
256 Due to the high affinity of HOCs for the organic carbon in soil, cosolvent-induced inhibition
257 of HOC sorption was more pronounced in soil with higher organic carbon content (i.e., S-3 in
258 contrast to S-1).

259 The sorption coefficients of PAHs increased with higher organic carbon content in batch
260 soil-water systems as illustrated in Table 2. The sorption coefficients of phenanthrene and
261 fluoranthene were the highest among the PAHs investigated. For the same PAH compound,
262 a reduction in PAH sorption from B1 to B20 was anticipated due to the lower PAH content of
263 biodiesel. On the other hand, with the addition of more biodiesel, the increased viscosity of
264 the biodiesel may inhibit the partitioning of PAHs from the soil phase into water. Previous
265 studies have indicated that viscosity affects the partitioning of PAHs from motor oil to the
266 water phase.²⁷ The influence of viscosity on rate may reflect the slower diffusion of
267 aromatic substrates in more viscous oils and their subsequent slower mass transfer to water.
268 Viscosity could also affect the rate of microbial utilization of petroleum hydrocarbons. The
269 rate and extent of biodegradation decrease with increasingly viscous nontoxic nonaqueous
270 phase liquids (NAPLs).²⁸ Given the combined effect of these two factors, the K_p values
271 showed a greater variation than those of ethanol-blended gasoline. Additionally, this
272 variation may depend on the composition of the soil's organic matter.²⁹⁻³¹ For the highly
273 hydrophobic PAHs, their concentration in solution is often relatively low. Thus, the

274 measured sorption coefficients risk being analytical artifacts, in particular, the measurements
275 of PAHs in aqueous phase. This may be the cause of low sorption coefficients for
276 fluoranthene and pyrene in S-1 observed in this study.

277 The sorption of a target compound is related to the organic carbon content of the soil.¹⁹
278 Examining the normalized sorption coefficients (K_{oc}) of BTEX and MTBE derived from K_p
279 in this study, the addition of ethanol leads to a decrease in K_{oc} (Table 3). Generally the K_{oc}
280 value correlates with the K_{ow} of target compounds. Careful determinations of nonionic
281 organic compound sorption from regular gasoline into natural organic matter appear to yield
282 log K_{oc} values that differ from previously reported values by approximately 0.37 to 0.96 log
283 units. The log K_{oc} value for MTBE indicates a low potential for sorption onto aquifer
284 material. The K_{oc} for BTEX in E85 was approximately 1.3 to 1.5 log units lower compared
285 to regular gasoline.

286 The sorption of PAHs in biodiesel onto soil is stronger comparing to BTEX and MTBE.
287 The sorption of HOCs from biodiesel is directly related to the organic carbon content of
288 different soils. It was observed that PAH sorption was approximately 3 to 5 times higher
289 with S-3 than S-1 (Table 2). The K_{oc} values for phenanthrene, fluoranthene, and pyrene
290 were the highest, whereas that for naphthalene was the lowest as anticipated (Table 3). In
291 Figure 1, the measured K_{oc} values are plotted versus the predicted values. Substantial
292 evidence has indicated that the equilibrium partitioning model may not be sufficient to
293 describe the sorption of HOCs in soil because organic matter is heterogeneous and sorption is
294 governed by nonequilibrium processes.^{30,31,33} K_{oc} values were found to vary up to a factor
295 of 100 between different soils and/or sediments.³¹ Therefore, the correspondence between
296 the measured and predicted K_{oc} values was considered to be acceptable. The empirical
297 relationship between K_{oc} and water solubility (S) and between K_{oc} and K_{ow} were established
298 as follows:

$$299 \quad \log K_{oc} = 0.6212 \log K_{ow} + 0.7919 \quad r^2 = 0.915 \quad (3)$$

$$300 \quad \log K_{oc} = -0.4172 \log S + 3.5475 \quad r^2 = 0.926 \quad (4)$$

301 These empirical equations will enable the sorption behavior of biofuel contaminants to be
302 quantitatively estimated in the event of a biofuel spill.

303

304 *Column experiments*

305 Liquid samples from the column effluent that interacted with biofuel-contaminated soil
306 were analyzed for target HOCs. In the case of a biofuel spill in the subsurface environment,
307 the aquifer may be contaminated with hydrophobic fuel constituents (e.g., aromatic compounds).
308 The initial residual biofuel saturation was calculated for each soil sample from the entrapped
309 volume of biofuel divided by the void volume of the column. This value ranged from 0.19
310 to 0.27 within columns contaminated with ethanol-blended gasoline, and from 0.38 to 0.41
311 within columns contaminated with biodiesel. It was found that the dissolution rate of biofuel
312 in the column experiments depends on the effective solubilities and diffusivities of the target
313 compounds, the physical distribution of the HOC in the porous medium, and the rate of water
314 flow through and around the biofuel. The rate of mass transfer determines the
315 dissolved-phase concentrations in the effluent water as well as the persistence of residual
316 biofuel constituents in the column. Higher water velocities may result in a reduction in the
317 dissolved concentrations.

318 In the case of dissolution from the residual phase, the local equilibrium concentration is
319 reached after short flow distances through the NAPL zone if the residual NAPL saturation is
320 high. Examining the breakthrough curves of the ethanol-blended gasoline constituents, MTBE
321 eluted in the first five pore volumes (PV) due to its partially miscible nature in groundwater.
322 The concentration of each constituent increased sharply over the first few pore volumes as
323 groundwater progressed through the column. In terms of eluted mass (concentration), the

324 difference was obvious for compounds such as MTBE and xylenes (Figure 2). Continuous
325 desorption of contaminants such as BTEX was observed until 50 PV in the ethanol-blended
326 gasoline spill site. Notably, elution times were longer for more hydrophobic contaminants.

327 The addition of ethanol enables gasoline constituents to enter smaller pore spaces and to
328 infiltrate more easily through the vadose zone to the water table. This effect is complicated
329 by strong ethanol partitioning to vadose-zone water, which significantly reduces ethanol
330 transport to the water table. Previous small-scale experiments have indicated that the loss of
331 ethanol before ethanol-blended gasoline reaches the water table does not significantly change
332 NAPL spreading on the capillary fringe or water table.³⁴ However, a large-volume spill of
333 E25 or E85 could overcome this effect and reach the water table, increasing the spreading of
334 NAPL. Our study indicated that the decreased sorption of hydrophobic contaminants causes
335 NAPL spreading, thereby increasing the extent of the dissolved contaminant plume and
336 contaminated area. In soil-water systems, the time to reach near-equilibrium conditions may
337 be on the scale of several days, particularly in desorption experiments. The breakthrough
338 concentration profile for each biofuel constituent was integrated over the cumulative effluent
339 volume (i.e., the zeroth moment) to determine the total HOC mass removed during the
340 experiment. Several parameters are necessary to allow such an evaluation: (1) the target
341 compound concentrations in the biofuel, which allows the amounts of MTBE, BTEX, and
342 PAHs that the biofuel puts in to the soil column to be estimated; (2) the amount of HOCs in
343 the effluent by using zero moment analysis on the elution profiles as illustrated in Figures 2
344 and 3 (using effluent concentration measurements of sixty pore volumes for ethanol-blended
345 gasoline 12 pore volumes for biodiesel). With these parameters, the net HOCs eluted can be
346 estimated with the following equation:

$$347 \quad \text{Eluted mass (\%)} = \text{HOC}_E / \text{HOC}_S \quad (5)$$

348 where HOC_E is the amount of HOCs in the effluent by using zero moment analysis on the
349 elution profiles as illustrated in Figures 2 and 3, and HOC_S is the original mass of HOCs in
350 the contaminated soil.

351 The moment analysis indicated that more desorbed target compounds were observed in
352 the effluent of E-85 than in regular gasoline. An effect of ethanol on the desorption of
353 xylenes was observed in the elution profiles of E-25 and E-85. The mass of xylenes
354 desorbed was greater in both E-85 and E-25 than in gasoline. Overall, the ethanol-induced
355 desorption of target compounds in high-ethanol content gasoline has the potential to increase
356 both the extent of contamination and the difficulty of remediation.

357 When groundwater encounters biodiesel-contaminated soil or aquifer material, the aqueous
358 concentrations of PAHs that previously sorbed onto the soil desorb according to their dissolution
359 rate. The effluent concentration increased and reached its maximum in the elution profile
360 during the first pore volume (Figure 3). Naphthalene and phenanthrene were selected to
361 show representative elution profiles. While groundwater was in contact with pure phase
362 NAPL, the NAPL in the pore space was displaced by groundwater flowing in. Therefore,
363 spikes in target compound concentrations were observed in the effluent as illustrated in
364 Figure 3. Our study indicated that the leaching of PAHs in column experiments appears to
365 be controlled by two major processes: the dissolution of PAHs from residual biodiesel and
366 desorption of PAHs from contaminated soil. Examining the elution profiles of biodiesel in
367 Figure 3, the elution of PAHs goes back to the normal dissolution rate after the first few pore
368 volumes. However, these biodiesel constituents will continuously contaminate groundwater
369 as long as groundwater passes through. The desorption of PAHs from soil with higher
370 organic carbon content tends to be slower ($S_3 < S_1$). Tailing of elution was observed while
371 residual biofuel existed in the subsurface environment. It should be noted that the spill
372 simulation conducted here only represents the scenario near the spill site. The effluent

373 measured is composed of PAHs from the dissolution of biofuel constituents from
374 contaminated soil. The dissolution of PAH components depends on chemical properties such
375 as hydrophobicity and total mass of biodiesel. Overall, the less-hydrophobic compounds elute
376 first, while the opposite is true for more-hydrophobic compounds.

377

378 **Conclusions**

379 Proposals for the modification of current fuels should include evaluations of the
380 constituents for their potential to damage environmental resources. The potential for
381 chemicals of concern to leach from biofuel-impacted soil must be understood to assess the
382 risk to groundwater. Knowledge of the sorption behavior of biofuel constituents is required
383 to ensure that the proper fate and transport of such contaminants is understood at
384 biofuel-contaminated sites.

385 Interactions such as sorption and desorption between dissolved organic species and
386 solids in the aquifer or soil depend on the physico-chemical parameters of the contaminant as
387 well as of those of the aquifer material. In this study, batch and column experiments were
388 designed to simulate biofuel spills in the subsurface environment and to evaluate the sorption
389 behavior of biofuel HOCs in soil. This study provides a rapid means of estimating the
390 potential for contamination from target compounds (i.e., monoaromatic and polyaromatic
391 hydrocarbons) and other organic contaminants from biofuels in various types of soil. The
392 extent and reversibility of the sorption of major components from biofuels onto major soil
393 types and groundwater were determined. The results showed that as the proportion of
394 ethanol in gasoline increased, the desorption of pollutants to water occurred more readily, an
395 effect that was obvious when the ethanol content exceeded 25%. However, if more
396 biodiesel was added to diesel fuel, the sorption of HOCs was not affected. In addition,
397 when the soil's organic carbon was higher, the desorption of target compounds was lower.

398 The empirical relationships between K_{oc} and both water solubility (S) and K_{ow} were
399 established. These empirical equations will allow the sorption behavior of biofuel
400 contaminants to be estimated in the event of a biofuel spill. The implication of this
401 experiment is that determining the sorption behavior and leaching patterns of major biofuel
402 constituents is important for future assessments of the impacts of biofuels. The spill
403 scenarios generated may assist in the assessment of biofuel-contaminated sites.

404

405 **Acknowledgments**

406 This study was supported by funds from Ministry of Science and Technology, Taiwan
407 (Project No. 97-2313-B-017-001-MY3).

408

409 **References**

- 410 1. S. E. Powers, C. S. Hunt, S. E. Heermann, H. X. Corseuil, D. Rice and P. J. J. Alvarez, The
411 transport and fate of ethanol and BTEX in groundwater contaminated by gasohol, *Crit. Rev.*
412 *Environ. Sci. Technol.*, 2001, **31**, 79-123.
- 413 2. J. G. Freitas and J. F. Barker, Oxygenated gasoline release in the unsaturated zone-part 1:
414 source zone behavior, *J. Contam. Hydrol.*, 2011, **126**, 153-166.
- 415 3. J. G. Freitas, B. Doulatyari, J. W. Molson and J. F. Barker, Oxygenated gasoline release in the
416 unsaturated zone-part 2: downgradient transport of ethanol and hydrocarbons, *J. Contam.*
417 *Hydrol.*, 2011, **125**, 70-85.
- 418 4. S. Firth, B. Hildenbrand and P. Morgan, Ethanol effects on the fate and transport of gasoline
419 constituents in the UK, *Sci. Total Environ.*, 2014, **485-486**, 705-710.
- 420 5. S. E. Heermann and S. E. Powers, Modeling the partitioning of BTEX in
421 water-reformulated gasoline systems containing ethanol, *J. Contam. Hydrol.*, 1998, **34**,
422 315-341.

- 423 6. G. Adam, K. Gamoh, D. G. Morris and H. Duncan, Effect of alcohol addition on the
424 movement of petroleum hydrocarbon fuels in soil, *Sci. Total Environ.*, 2002, **286**, 15-25.
- 425 7. H. X. Corseuil, B. I. A. Kaipper and M. Fernandes, Cosolvency effect in subsurface
426 systems contaminated with petroleum hydrocarbons and ethanol, *Water Res.*, 2004, **38**,
427 1449-1456.
- 428 8. C. S. Chen, Y.-W. Lai and C.-J. Tien, Partitioning of aromatic and oxygenated constituents
429 into water from regular and ethanol-blended gasolines, *Environ. Pollut.*, 2008, **156**, 988-996.
- 430 9. M. L. B. Da Silva and P. J. J. Alvarez, Effects of ethanol versus MTBE on benzene,
431 toluene, ethylbenzene, and xylene natural attenuation in aquifer columns, *J. Environ. Eng.*,
432 2002, **128**, 862-867.
- 433 10. N. Lovanh, C. S. Hunt and P. J. J. Alvarez, Effect of ethanol on BTEX biodegradation
434 kinetics: aerobic continuous culture experiments, *Water Res.*, 2002, **36**, 3739-3746.
- 435 11. D. M. Mackay, N. R. De Sieyes, M. D. Einarson, K. P. Peris, A. A. Pappas, I. A. Wood, L.
436 Jacobson, L. G. Justice, M. N. Noske, K. M. Scow and J. T. Wilson, Impact of ethanol on the
437 natural attenuation of benzene, toluene, and o-xylene in a normally sulfate-reducing aquifer,
438 *Environ. Sci. Technol.*, 2006, **40**, 6123-6130.
- 439 12. K. Feris, D. Mackay, N. De Sieyes, I. Chakraborty, M. Einarson, K. Hristova and K.
440 Scow, Effect of ethanol on microbial community structure and function during natural
441 attenuation of benzene, toluene, ethylbenzene, and o-xylene in a sulfate-reducing aquifer,
442 *Environ. Sci. Technol.*, 2008, **42**, 2289-2294.
- 443 13. C. S. Chen, Y.-W. Lai and C.-J. Tien, Partitioning of polynuclear aromatic hydrocarbons
444 into water from biodiesel fuel mixtures, *Environ. Chem.*, 2008, **5**, 435-444.
- 445 14. G. W. Gee and J. W. Bauder, in *Methods of Soil Analysis, Part 1*, ed. A. Klute, Soil Science
446 Society of America, Madison, 2nd edn, 1986, pp.383-411.
- 447 15. C. S. Chen, P. S. C. Rao and L. S. Lee, Evaluation of extraction and analytical methods

- 448 for determining polynuclear aromatic hydrocarbons from coal tar contaminated soils,
449 *Chemosphere*, 1996, **32**, 1123-1132.
- 450 16. L. S. Lee, P. S. C. Rao, M. L. Brusseau and R. A. Ogwada, Nonequilibrium sorption of
451 organic contaminants during flow through columns of aquifer material, *Environ. Toxicol. Chem.*,
452 1988, **7**, 779-793.
- 453 17. M. L. Brusseau, R. E. Jessup and P. S. C. Rao, Sorption kinetics of organic chemicals:
454 evaluation of gas-purge and miscible-displacement techniques. *Environ. Sci. Technol.*, 1990, **24**,
455 727-735.
- 456 18. R. P. Schwarzenbach, P. M. Gschwend and D. M. Imboden, *Environmental Organic*
457 *Chemistry*. 2003, 2nd Eds., New York, Wiley-Interscience.
- 458 19. S. W. Karickhoff, D. S. Brown and T. A. Scott, Sorption of hydrophobic pollutants on natural
459 sediments, *Water Res.*, 1979, **13**, 241-248.
- 460 20. S. B. F. Reckhorn, L.V. Zuquette and P. Grathwohl, Experimental investigations of
461 oxygenated gasoline dissolution, *J. Environ. Eng.*, 2001, **127**, 208-216.
- 462 21. P. Nkedi-Kizza, P. S. C. Rao and A. G. Hornsby, Nonequilibrium sorption during
463 displacement of hydrophobic organic chemicals and Ca⁴⁵ through soil columns with aqueous
464 and mixed solvents, *Environ. Sci. Technol.*, 1989, **23**, 814-820.
- 465 22. M. L. Brusseau, A. L. Wood and P. S. C. Rao, Influence of organic cosolvents on the
466 sorption kinetics of hydrophobic organic chemicals, *Environ. Sci. Technol.*, 1991, **25**,
467 903-910.
- 468 23. D. C. M. Augustijn, R. E. Jessup, P. S. C. Rao, and A. L. Wood, Remediation of
469 contaminated soils by solvent flushing, *J. Environ. Eng.*, 1994, **120**, 42-57.
- 470 24. C. S. Chen, P. S. C. Rao and J. J. Delfino, Cosolvent induced dissolution of polynuclear
471 aromatic hydrocarbons due to spills of oxygenated fuels in the subsurface environment,
472 *Chemosphere*, 2005, **60**, 1572-1582.

- 473 25. S. H. Yalkowsky and J. T. Rubino, Solubilization by Cosolvents I: Organic Solutes in
474 Propylene Glycol-Water Mixture, *J. Pharm. Sci.*, 1985, **74**, 416-421.
- 475 26. P.S.C. Rao, L.S. Lee and R. Pinal, Cosolvency and sorption of hydrophobic organic
476 chemicals, *Environ. Sci. Technol.*, 1990, **24**, 647-654.
- 477 27. C. S. Chen, J. J. Delfino and P. S. C. Rao, Partitioning of organic and inorganic pollutants
478 from motor oil into water, *Chemosphere*, 1994, **28**, 1385-1400.
- 479 28. I. Birman and M. Alexander, Effect of viscosity of nonaqueous liquids (NAPLs) on
480 biodegradation of NAPL constituents, *Environ. Toxicol. Chem.* 1996, **15**, 1683-1686.
- 481 29. D. E. Kile, R. L. Wershaw and C. T. Chiou, Correlation of soil and sediment organic
482 matter polarity to aqueous sorption of nonionic compounds, *Environ. Sci. Technol.*, 1999, **33**,
483 2053-2056.
- 484 30. A. D. Lueking, W. Huang, S. Soderstrom-Schwarz, M. Kim and W.J. Weber, Jr.,
485 Relationship of Soil Organic Matter Characteristics to Organic Contaminant Sequestration and
486 Bioavailability, *J. Environ. Qual.*, 2000, **29**, 317-323.
- 487 31. M. Krauss and W. Wilcke, Predicting soil-water partitioning of polycyclic aromatic
488 hydrocarbons and polychlorinated biphenyls by desorption with methanol-water mixtures at
489 different temperatures, *Environ. Sci. Technol.*, 2001, **35**, 2319-2325.
- 490 32. J. H. Montgomery, *Groundwater chemicals desk reference*, 4th edn, CRC Press, Florida,
491 2007.
- 492 33. J. J. Pignatello and B. Xing, Mechanisms of slow sorption of organic chemicals to natural
493 particles, *Environ. Sci. Technol.*, 1996, **30**, 1-11.
- 494 34. C. J. McDowell and S. E. Powers, Mechanisms affecting the infiltration and distribution
495 of ethanol-blended gasoline in the vadose zone, *Environ. Sci. Technol.*, 2003, **37**, 1803-1810.

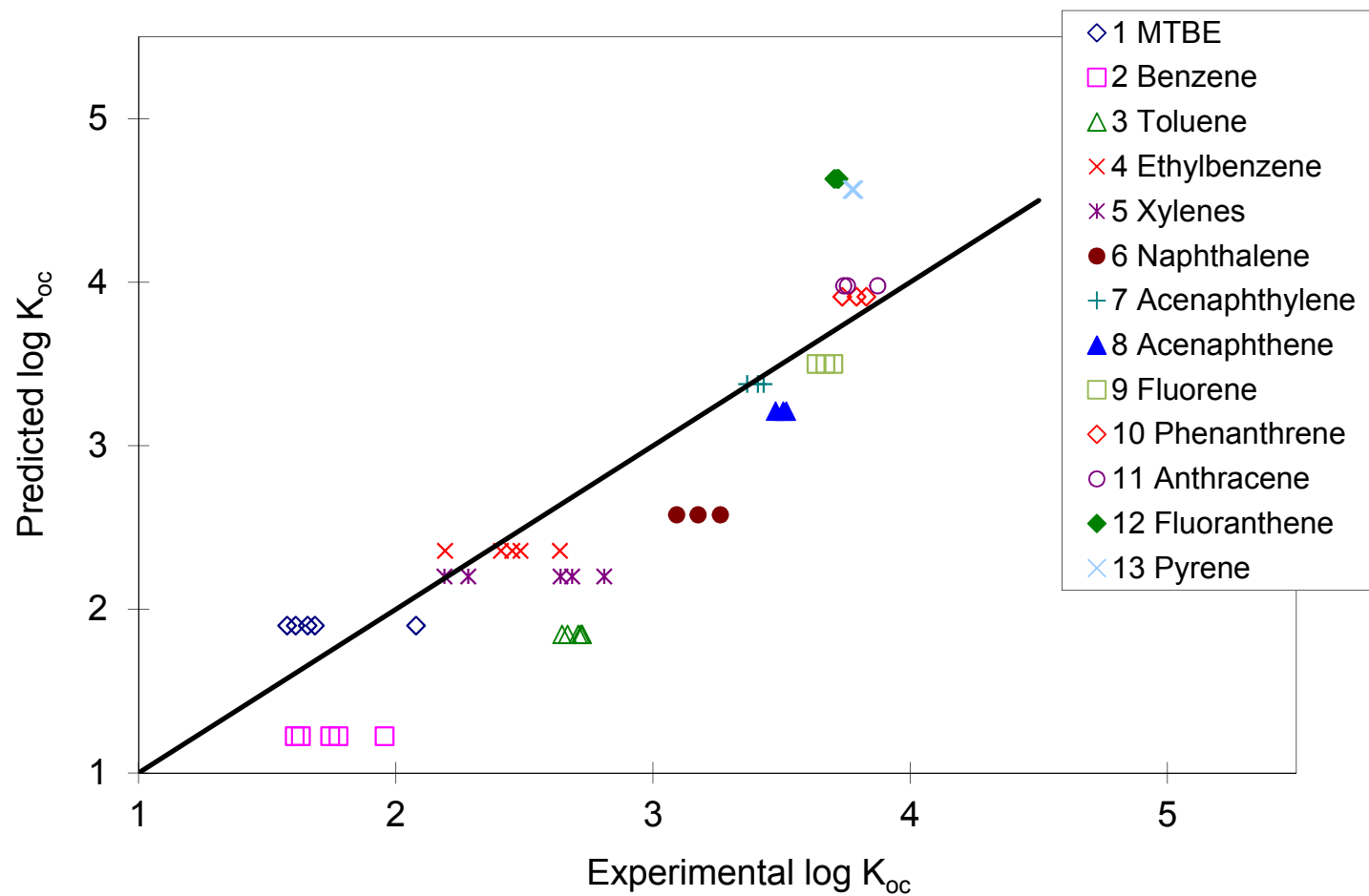


Figure 1. Experimental vs. predicted $\log K_{oc}$ values for target compounds in biofuel.

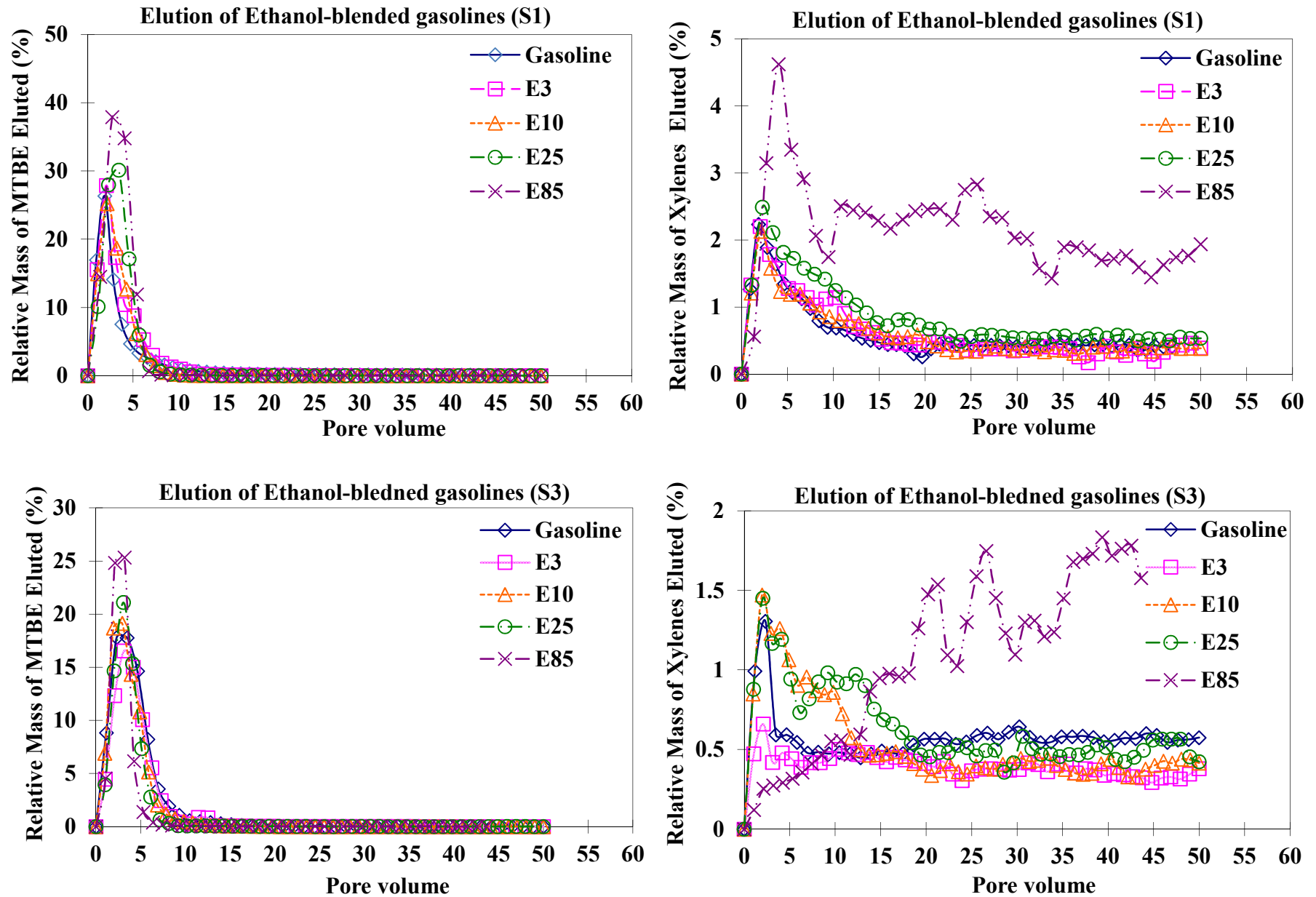


Figure 2. The elution profile of MTBE and xylenes in various gasoline products.

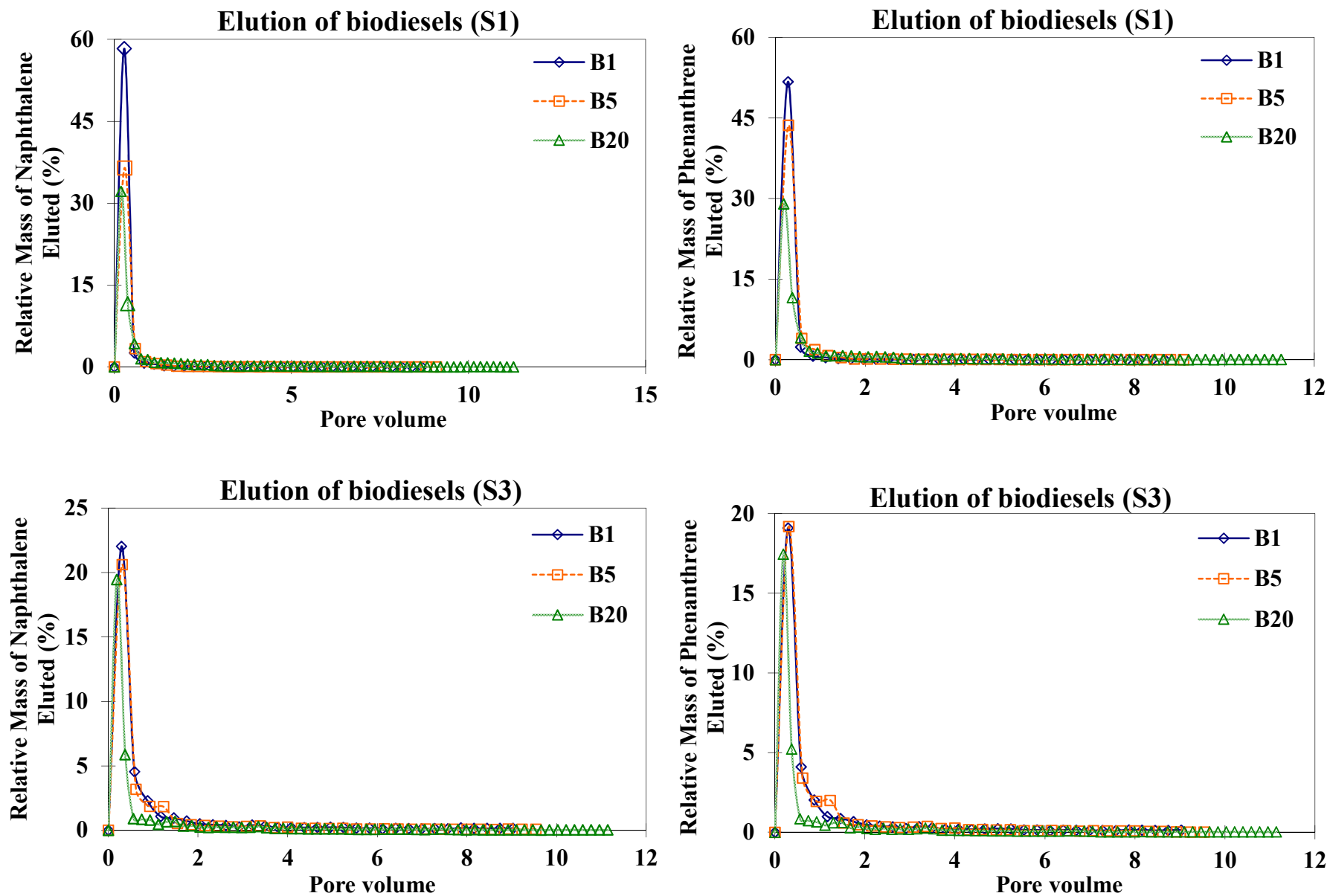


Figure 3. The elution profile of naphthalene and phenanthrene in various soils.

Table 1. The sorption coefficients (K_p) of target compounds in the ethanol-blended gasoline contaminated soil-water system.

| Compound | S1 ($f_{oc}=2.6\%$) (Fuel/soil=1:10) | | | | | S1 ($f_{oc}=2.6\%$) (Fuel/soil=1:1) | | | | |
|----------|--|------|---------|---------|--------------|---------------------------------------|-------|---------|---------|--------------|
| | Fuel | MTBE | Benzene | Toluene | Ethylbenzene | Xylenes | MTBE | Benzene | Toluene | Ethylbenzene |
| CPC95 | 7.93 | 45.8 | 70.7 | 45.8 | 74.9 | 0.676 | 12.6 | 10.9 | 15.9 | 14.7 |
| E3 | 12.7 | 43.0 | 63.1 | 37.0 | 49.9 | 0.542 | 10.0 | 9.65 | 13.7 | 12.2 |
| E10 | 9.08 | 37.7 | 92.8 | 40.9 | 60.3 | 0.521 | 7.35 | 5.20 | 10.4 | 6.94 |
| E25 | 5.54 | 39.2 | 80.7 | 69.9 | 83.6 | 0.390 | 1.55 | 2.36 | 3.47 | 2.24 |
| E85 | 4.16 | 42.1 | 21.1 | 42.6 | 30.9 | 0.346 | 1.04 | 1.02 | 2.02 | 1.98 |
| | S2 ($f_{oc}=4.5\%$) | | | | | S2 ($f_{oc}=4.5\%$) | | | | |
| CPC95 | 15. | 53.5 | 81.5 | 52.4 | 74.8 | 0.721 | 22.7 | 23.5 | 45.0 | 39.5 |
| E3 | 24.0 | 45.8 | 106 | 44.1 | 68.8 | 0.708 | 15.1 | 11.6 | 9.91 | 10.7 |
| E10 | 11.4 | 37.8 | 154 | 43.0 | 62.6 | 0.661 | 14.2 | 8.06 | 16.1 | 12.1 |
| E25 | 7.25 | 39.1 | 110 | 67.5 | 91.8 | 0.303 | 1.27 | 1.71 | 4.07 | 3.24 |
| E85 | 7.57 | 42.9 | 25.4 | 60.9 | 58.6 | 0.208 | 0.671 | 0.732 | 1.72 | 1.41 |
| | S3 ($f_{oc}=10.0\%$) | | | | | S3 ($f_{oc}=10.0\%$) | | | | |
| CPC95 | 18.3 | 51.8 | 110 | 58.3 | 88.0 | 4.24 | 70.0 | 95.4 | 100 | 123 |
| E3 | 18.6 | 47.9 | 110 | 56.6 | 85.2 | 4.15 | 65.3 | 90.3 | 90.2 | 122 |
| E10 | 12.8 | 40.7 | 142 | 62.5 | 94.3 | 3.51 | 31.4 | 32.1 | 39.4 | 36.2 |
| E25 | 8.62 | 41.9 | 119 | 88.7 | 96.5 | 1.63 | 6.80 | 14.9 | 23.8 | 25.9 |
| E85 | 8.44 | 48.5 | 58.3 | 77.5 | 83.0 | 0.245 | 0.791 | 0.798 | 0.912 | 1.24 |

Table 2. The sorption coefficients (K_p) of target compounds in the biodiesel contaminated soil-water system.

| Compound Biodiesel | S1 ($f_{oc}=2.6\%$) | | | | | | | |
|-----------------------|-----------------------|----------------|--------------|----------|--------------|------------|--------------|--------|
| | Naphthalene | Acenaphthylene | Acenaphthene | Fluorene | Phenanthrene | Anthracene | Fluoranthene | Pyrene |
| B1 | 25.11 | 70.87 | 89.84 | 80.13 | 183.7 | 117.5 | 195.7 | 141.6 |
| B5 | 27.46 | 81.67 | 115.7 | 116.1 | 180.8 | 127.0 | 169.1 | 132.2 |
| B20 | 43.51 | 91.42 | 116.6 | 94.13 | 156.7 | 113.2 | 197.9 | 139.3 |

| Compound Biodiesel | S2 ($f_{oc}=4.5\%$) | | | | | | | |
|-----------------------|-----------------------|----------------|--------------|----------|--------------|------------|--------------|--------|
| | Naphthalene | Acenaphthylene | Acenaphthene | Fluorene | Phenanthrene | Anthracene | Fluoranthene | Pyrene |
| B1 | 89.04 | 81.85 | 96.01 | 157.4 | 210.6 | 165.9 | 272.4 | 189.0 |
| B5 | 85.57 | 128.5 | 129.6 | 175.9 | 213.7 | 157.1 | 363.2 | 157.0 |
| B20 | 83.86 | 113.0 | 150.6 | 153.7 | 293.2 | 192.7 | 269.4 | 183.0 |

| Compound Biodiesel | S3 ($f_{oc}=10.0\%$) | | | | | | | |
|-----------------------|------------------------|----------------|--------------|----------|--------------|------------|--------------|--------|
| | Naphthalene | Acenaphthylene | Acenaphthene | Fluorene | Phenanthrene | Anthracene | Fluoranthene | Pyrene |
| B1 | 145.8 | 211.8 | 264.8 | 423.0 | 555.3 | 522.8 | 386.2 | 535.3 |
| B5 | 128.5 | 288.8 | 281.3 | 435.6 | 514.7 | 547.9 | 388.3 | 447.2 |
| B20 | 140.3 | 213.1 | 352.8 | 434.6 | 440.8 | 513.7 | 373.0 | 440.8 |

Table 3. The K_{oc} values of target compounds in biofuels.

A. Ethanol-blended gasoline

| Biofuel Compound | CPC95 | | E3 | | E10 | | E25 | | E85 | | Previous studies ^a |
|---------------------|----------|--------------|----------|--------------|----------|--------------|----------|--------------|----------|--------------|-------------------------------|
| | K_{oc} | log K_{oc} | log K_{oc} |
| MTBE | 28.2 | 1.45 | 26.0 | 1.42 | 23.3 | 1.37 | 12.7 | 1.10 | 6.11 | 0.791 | 1.08 |
| Benzene | 563 | 2.75 | 458 | 2.66 | 304 | 2.48 | 52.0 | 1.72 | 19.6 | 1.29 | 2.00 |
| Toluene | 632 | 2.80 | 511 | 2.71 | 234 | 2.37 | 92.6 | 1.97 | 20.8 | 1.32 | 2.06 |
| Ethylbenzene | 870 | 2.94 | 595 | 2.77 | 315 | 2.50 | 154 | 2.19 | 40.6 | 1.61 | 1.98, 2.41 |
| Xylenes | 890 | 2.95 | 654 | 2.82 | 299 | 2.48 | 152 | 2.18 | 44.2 | 1.65 | 2.11, 2.31 |

^a From [32].

B. Biodiesel

| Biofuel Compound | B1 | | B5 | | B20 | | Previous Studies ^a |
|---------------------|----------|---------------|----------|---------------|----------|---------------|-------------------------------|
| | K_{oc} | $\log K_{oc}$ | K_{oc} | $\log K_{oc}$ | K_{oc} | $\log K_{oc}$ | $\log K_{oc}$ |
| Naphthalene | 1497 | 3.18 | 1235 | 3.09 | 1827 | 3.26 | 3.11 |
| Acenaphthylene | 2694 | 3.43 | 2324 | 3.37 | 2557 | 3.41 | 3.40 |
| Acenaphthene | 3209 | 3.51 | 3299 | 3.52 | 2999 | 3.48 | 3.66 |
| Fluorene | 4677 | 3.67 | 4326 | 3.64 | 5029 | 3.70 | 3.70, 3.86 |
| Phenanthrene | 6756 | 3.83 | 6182 | 3.79 | 5443 | 3.74 | 4.15, 4.36 |
| Anthracene | 5703 | 3.76 | 7460 | 3.87 | 5507 | 3.74 | 4.15, 4.27 |
| Fluoranthene | 5267 | 3.72 | 5195 | 3.72 | 5065 | 3.70 | 4.58, 4.62 |
| Pyrene | 6016 | 3.78 | 5828 | 3.77 | 6040 | 3.78 | 4.58, 4.81 |

a From [32].